Image Correlation Applied to Single Crystal Plasticity Experiments and Comparison to Strain Gage Data

M. M. LeBlanc, J. N. Florando, D. H. Lassila, T. Schmidt, J. Tyson II

July 13, 2005

Experimental Techniques

Disclaimer

Image Correlation Applied to Single Crystal Plasticity Experiments and Comparison to Strain Gage Data

By M.M. LeBlanc, J.N. Florando, D.H. Lassila, T. Schmidt, J. Tyson II

Full-field optical techniques are becoming increasingly popular for measuring the deformation of materials, especially in materials that exhibit non-uniform behavior. While there are many full-field techniques available (e.g. moiré interferometry, electronic speckle pattern interferometry (ESPI)**,** holography**,** and image correlation [1]), for our study of the deformation of single crystals, the image correlation technique was chosen for its insensitivity to vibrations and ability to measure large strains. While the theory and development of the algorithms for image correlation have been presented elsewhere [2,3] a comparative study to a conventional strain measurement device, such as a strain gage rosette, is desired to test the robustness and accuracy of the technique.

The 6 Degrees of Freedom (6DOF) experiment, which was specifically designed to validate dislocation dynamics (DD) simulations [4], is ideally suited to compare the two methods. This experiment is different from previous experiments on single crystals in that it allows the crystal to deform essentially unconstrained, in both the elastic and plastic regimes, by allowing the bottom of the sample to move as the sample is being compressed. This unconstrained motion prevents the internal crystal planes from rotating during the deformation as typically seen in the pioneering work of Schmid [5] and Taylor [6]. In the early development of the 6DOF apparatus, stacked strain gage rosettes were used to provide the strain data [7]. While very accurate at small strains, strain gages provide an averaged measurement over a small area and cannot be used to measure the inhomogeneous plastic strains that typically occur during the 6DOF experiment. An image correlation technique can measure the full-field in-plane and out-of-plane deformation that occurs in single crystals, and a comparison to the strain gage data at small strains can test the accuracy of the method.

The 6 DOF experiment

The 6DOF experiment, as shown in Fig. 1, allows the sample to deform with minimal constraint in 6 directions. The sample is compressed along the z-axis by loading the half sphere, which allows the sample to tilt in two directions. The sample is attached to a platen that sits on ball bearings, which allows the sample bottom to translate freely and rotate in the x-y plane, giving it 6 degrees of freedom.

In our early experiments, stacked rosette strain gages (MicroMeasurements SA-06-030WR-120) were bonded to the center of the four faces of the sample[1]. The resolution of the gages at small strains (on the order of 20-30 microstrain) permits measurement of the anisotropic elastic constants of the single crystal sample. At larger strains there are two main limitations of the gages. Strain gages provide a single measurement over a small area (active region is 0.75 mm by 0.75 mm), and therefore inhomogeneities in the strain cannot be measured. Also, the stacked strain gages rosettes have a working range up to only 1.5% - 2.0% strain.

Image correlation can be used to measure the full-field strains up to hundreds of percent. The premise behind image correlation is that images of a stochastic pattern on the sample (typically black dots on a white background for the highest contrast) are recorded with a CCD camera during deformation. The images are then compared, and the relative movement and shape change of the dots in relation to one another gives local displacements that can be used to calculate strain. By using a pair of cameras, both in-plane and out-of-plane displacements can be measured. The resolution of the system is dependant upon the number of pixels in the CCD camera, the field of view, and the number of pixels used for the calculation of the strain.

The specific system used in this study is the GOM ARAMIS 3D image correlation photogrammetry system with two pairs of 1.3 megapixel cameras, and a field of view of 20 mm x 25 mm. In order to calculate the local deformation gradient, an area of pixels, called a facet, must be defined. The facet size used is 19 pixels with a step of 12, which

---

[1] The 6DOF experiment with strain gages uses many additional diagnostics to measure the sample deformation: four laser triangulation sensors track the translation and rotation of the translation platen, a fifth laser sensor measures rotation of the half sphere, three extensometers measure the tilt of the half sphere, and two diametral extensometers attached to the corners of the sample measure the out-of-plane shear strains.

means the distance between the centers of two adjacent facets is 12 pixels. The virtual strain length, which is the smallest distance that the local strain is calculated over, is 33 pixels by 33 pixels, or 640 μm by 640 μm. Using a 3 x 5 median filter, this set-up has a displacement resolution of 0.5 μm, and an experimental strain noise floor of about 100 microstrain.

For the experimental set-up using image correlation, Fig. 2, two camera pairs are synced together to obtain data on two adjacent faces during loading. A pair of cameras is used for each face to triangulate the positions and calculate the 3D shape change in the sample. In order to account for rigid body translations in the displacement data, reference flags are attached to the translation platen and move with the sample. Since these flags do not deform, they can be used to eliminate the rigid body displacements and obtain accurate in-plane and out-of plane displacements. A pair of laser sensors is used to track the motion of the translation platen in real-time, and to compare with the image correlation data.

Experimental results

Two molybdenum single crystals samples (5 mm by 5mm wide and 15 mm tall) oriented with the $\left[\overline{2}\,9\,20\right]$ direction pointing in the positive z-direction are compressed in this study: one instrumented with strain gages and compressed to 0.006 axial strain and the other patterned for image correlation and compressed to 0.018 axial strain. The asymmetric orientation was chosen because its deformation behavior leads to a translation of the bottom platen in the 6DOF apparatus.

The stress-strain data from the strain-gaged sample is shown in Fig. 3a. The axial, transverse, and shear strains were measured with the strain gage rosettes, and the values from opposing faces were averaged. The error bars represent the spread in the data between opposite sides of the sample. The out-of-plane shear strains were measured with diametral extensometers so that the complete strain tensor could be calculated. The amount of tilt in the sample after 0.006 axial strain was measured to be 0.1 degrees, and the translation of the sample bottom was calculated to be 45 μm in the x-direction and 150 μm in the y-direction as shown in Fig. 3b. This calculation, using the equations in

Fig. 3b, assumes that the shear strains are uniform over the entire effective gage length, L_{eff}, which for this sample is 13.1 mm.

The axial stress-strain data from the image correlation experiment is shown in Fig. 4a. Also shown are the full-field axial strain maps, which indicate that the strains are fairly uniform along the face, with some regions of non-uniformity near the ends due to the boundary conditions. The shear and transverse strains, which are not shown, can also be displayed in a similar manner.

The in-plane and out-of-plane displacements on the sample faces are measured by removing the rigid body components of the displacement data. The in-plane displacement maps for two adjacent faces of the sample at the completion of the test are shown in Fig 4b. The relative motion of the bottom of the sample with respect to the top can be determined from the displacement maps. This technique is more precise than the strain gage calculation, because image correlation directly measures the motion of the sample. As shown in Fig 4b, the sample bottom moved 55 μm in the x-direction and 270 μm in the y-direction.

A comparison of the axial stress-strain data from the two techniques is shown in Fig. 5a. In order to compare the image correlation technique with the strain gages, the strains are averaged over an area similar in size and location on the sample to the active region of the strain gage. The results show a close agreement between the two techniques with the image correlation experiment achieving larger strains. Fig. 5b shows that for the three shear strain components, the strain gage data and the image correlation data are also are closely matched in the small strain regime. Finally, the results of the calculated sample translation are compared with the displacement of the sample measured with image correlation in Fig. 6. The difference between the two is likely due to the combined effects of the non-uniformity of the shear strains along the sample and the ambiguity in the assumed gage length of the sample.

Advantages of image correlation

In addition to measuring larger, full-field strains and tracking the motion of the sample, there is another advantage to using the image correlation technique which makes it an essential tool in studying the deformation of single crystals.

For single crystals in which there are multiple slip systems active, it is possible to calculate the activity of each slip system [8, 9] if the active slip systems and the full deformation tensor are known. The active slip systems can be determined from optical or other characterization techniques. A combination of strain gages on all faces and diametral extensometers, as shown in ref [9], allows for the full strain tensor to be determined. The shear strains, however, are the average of the two shear displacement gradient components,

$$\varepsilon_{yz} = \frac{1}{2}\left(\frac{du_y}{dz} + \frac{du_z}{dy}\right). \qquad (1)$$

Therefore, with the strain gage data, a unique solution of the slip system shear strains for up to only five independent slip systems can be obtained.

A more complete picture of the deformation is found in the nine components of the displacement gradient tensor. Since image correlation measures displacements, it is possible to obtain the full displacement gradient tensor, from which the slip activity for up to eight independent slip systems can be calculated. The displacement gradients are calculated by taking the slope of the displacement in one direction with respect to the other. For instance, the y-displacement as a function of z is shown in Fig. 7, and the slope of that line is a measure of $\frac{du_y}{dz}$ along that section line.

In the special case where the crystal is oriented such that the slip direction is parallel to a face of the sample, the slip activity for that slip system can be directly measured. Image correlation allows for the reference axes be rotated to look at displacements in the rotated coordinate system. By rotating one of the axes to lie along the slip direction, and using the same technique as shown in Fig. 7, a direct measurement of the slip activity can be made. This data is essential in directly comparing with DD simulations.

Conclusions

The results from compression tests on Mo single crystals using the 6DOF apparatus show that at small strains the image correlation system is able to match the data measured

using conventional strain gages. In addition, the image correlation technique has several advantages, such as the ability to measure large strains, full-field strains and displacement gradients, which make it an essential tool in measuring the deformation behavior of single crystals.

Acknowledgements

References

1. Cloud, G., "Optical Methods of Engineering Analysis," Cambridge University Press (1995).
2. Peters, W.H. and Ranson, W.F., "Digital imaging techniques in experimental stress analysis," *Optical Eng.*, 21(3), 427-431 (1982).
3. Schmidt, T., Tyson, J., and Galanulis, K., "Full-field dynamic displacement and strain measurement - specific examples using advanced 3D image correlation photogrammetry. Part II," *Exp. Tech.*, 27(4), 22-26 (2003).
4. Florando, J.N., LeBlanc, M.M., and Lassila, D.H., "Single Crystal Deformation Experiments using a "6 Degrees of Freedom" Apparatus," *submitted to Metallurgical Transactions*, (2005).
5. Schmid, E. and Boas, I.W., "Plasticity of Crystals," London: Chapman and Hall LTD (1950).
6. Taylor, G.I. and Farren, W.S., "The Distortion of Crystals of Aluminium under Compression Part I.," *Roy Soc. Proc. A*, 111A, 529-551 (1926).
7. Lassila, D.H., LeBlanc, M.M., and Kay, G.J., "Uniaxial stress deformation experiment for validation of 3-D dislocation dynamics simulations," *J. Eng. Mat. & Tech.-Trans. of the ASME*, 124(3), 290-296 (2002).
8. Havner, K.S. and Baker, G.S., "Theoretical latent hardening in crystals. II. BCC crystals in tension and compression," *J. Mech. Phys. Solids*, 27(4), 285-314 (1979).
9. Lassila, D.H., LeBlanc, M.M., and Rhee, M. "Single crystal deformation experiments for validation of dislocation dynamics simulations." Multiscale Phenomena in Materials - Experiments and Modeling Related to Mechanical Behavior Symposium. *Mater. Res. Soc. Symp. Proc.* 779, 37-48 (2003).
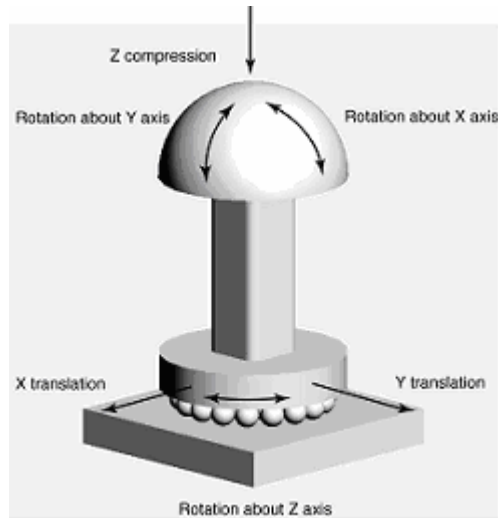
Figure 1-6DOF experiment. When the sample is compressed in the z direction, the half sphere on top of the sample is free to tilt and the bottom of the sample is able to freely translate and rotate.
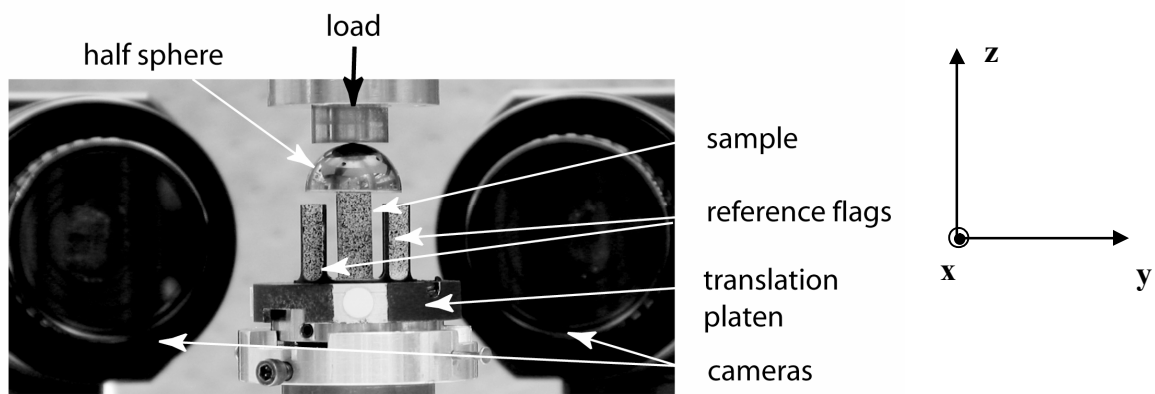

Figure 2-Experimental set-up using the GOM ARAMIS 3-D image correlation system. The reference flags and the bottom of the sample are both fixed to the translation platen. Because the flags to not deform during the experiment, they can be used to remove rigid body components from the in-plane and out-of-plane sample displacement data.

$$\delta_x = \gamma_{xz} \cdot L_{eff}$$

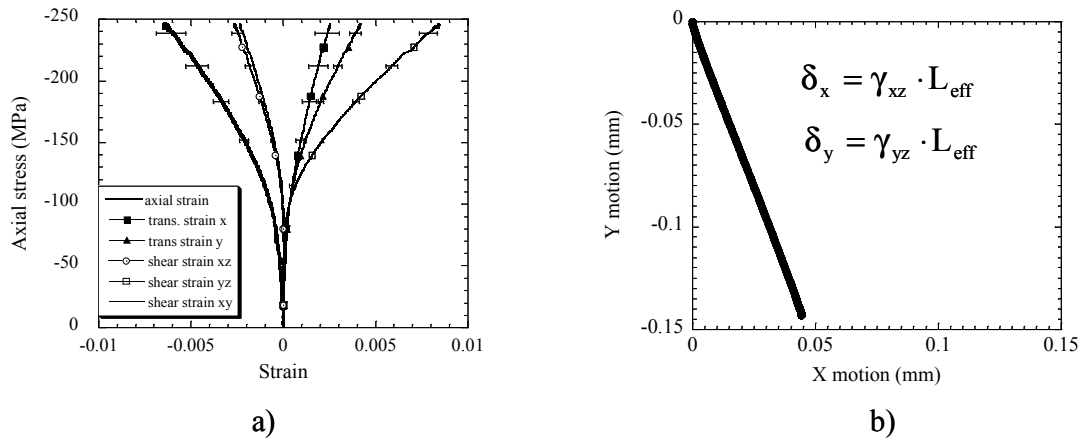$$\delta_y = \gamma_{yz} \cdot L_{eff}$$

a)

b)

Figure 3-Data from the strain-gaged sample.   a) All six strain components are plotted as a function of axial stress. The axial strain is the average of that measured on the four sides of the sample. The shear and transverse strains shown are the average of opposite sides of the sample. The error bars show the spread of the data from the average. The in-plane shear strain is calculated from two diametral extensometers placed across the corners of the sample. b) Translation of the bottom of the sample assuming the measured shears are uniform over the effective gage section of the sample.
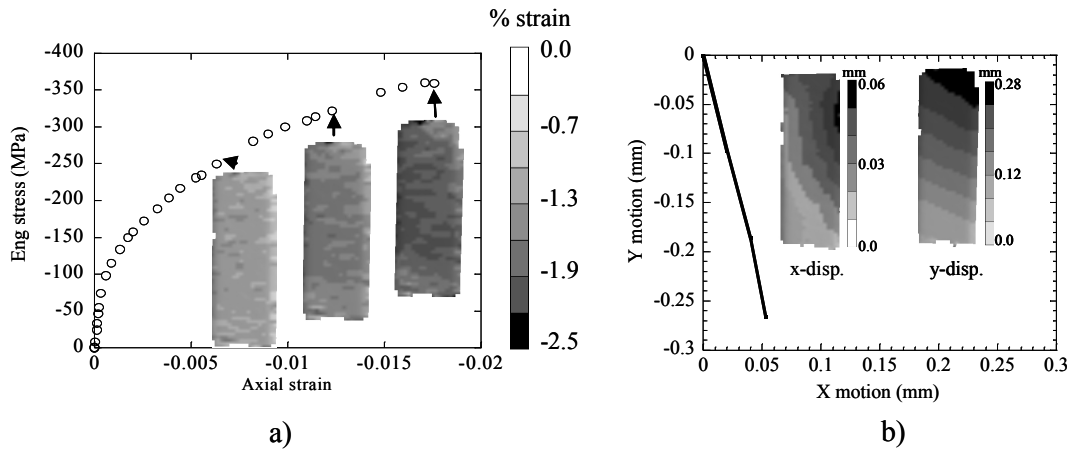
a)

b)

Figure 4-Image correlation data a) Axial stress-strain with snapshots showing full-field strains b) Movement of the bottom of the crystal in relation to the top calculated from the in-plane sample displacements.
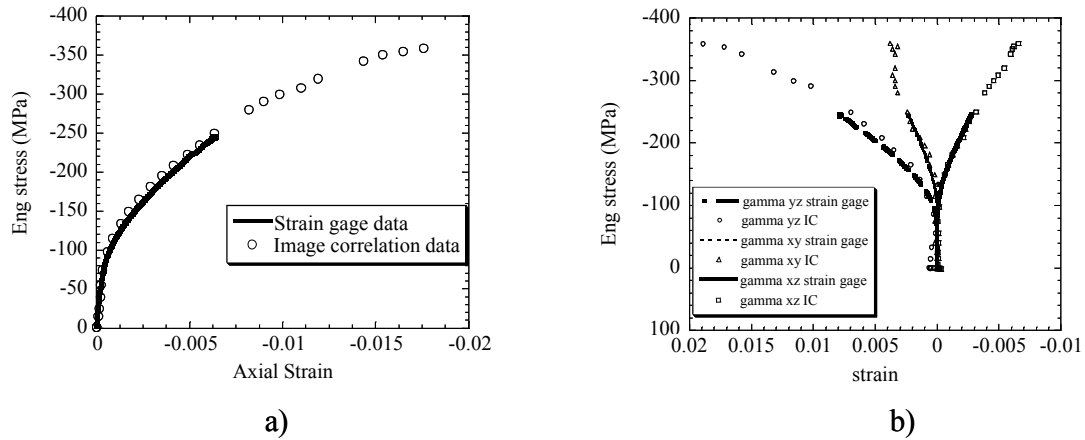
a)

b)

Figure 5-Comparison of the image correlation and strain gage data. a) axial stress vs. axial strain, b) axial stress vs. 3 shear strain components (γ_{yz}, γ_{xz}, γ_{xy})
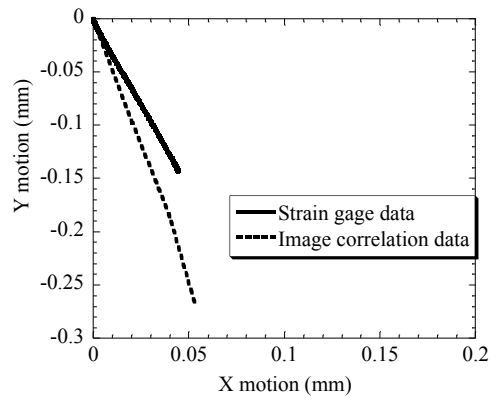

Figure 6- Comparison of the translations of the sample calculated from strain gages (0.006 axial strain) and measured using image correlation (0.018 axial strain). The difference between slopes is likely due to the combined effects of the non-uniformity of the shear strains along the samples, and ambiguity in the effective gage length. For the strain gage data, the translation is calculated from the average shear strains, while the image correlation technique provides a direct measurement of the x and y displacements.
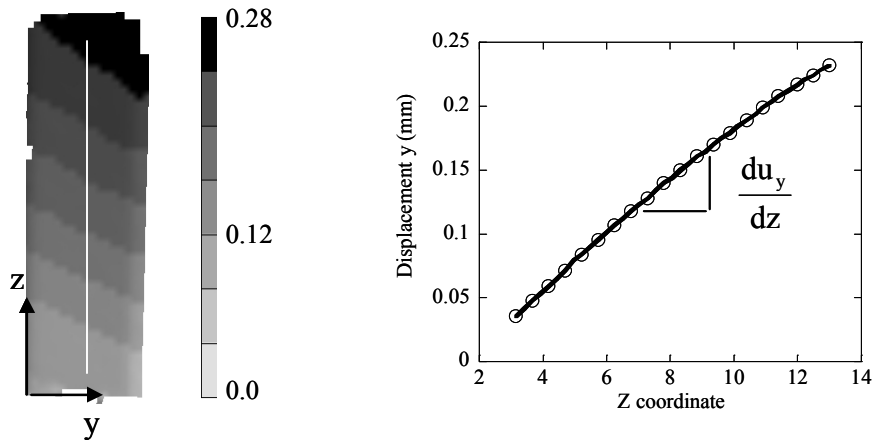
Figure 7-The y displacement plotted as a function of the z coordinate. The slope of the line is one component, du_y/dz, of the displacement gradient tensor.